

Effects of Tropical Rainfall to the Ku-Band Satellite Communications Links at the Equatorial Atmosphere Radar Observatory

Yasuyuki MAEKAWA, Tadashi FUJIWARA¹, Yoshiaki SHIBAGAKI

Dept. of Telecommunications and Computer Networks, Osaka Electro-Communication University, Neyagawa, Japan

Toru SATO

Graduate School of Informatics, Kyoto University, Kyoto, Japan

Mamoru YAMAMOTO, Hiroyuki HASHIGUCHI, and Shoichiro FUKAO

Research Institute for Sustainable Humanosphere, Kyoto University, Uji, Japan

(Manuscript received 19 November 2005, in final form 10 March 2006)

Abstract

This study investigates the effects of tropical rainfall on the Ku-band satellite communications links that connect Research Institute for Sustainable Humanosphere (RISH), Kyoto University in Japan to Equatorial Atmosphere Radar Observatory (EAR; 0.2°S, 100.3°E) in Indonesia, using the satellite Superbird C (144°E in orbit). Rain attenuation of the up- and down-link radio wave signals is, for the first time, obtained at the same time in the tropics, monitoring each signal level that has been received at both stations in Japan and Indonesia for the past three years from 2003 to 2005. The up-link attenuation at each station can be estimated from the down-link signal level measured at its opposite station, because SCPC (Single Channel Per Carrier) signals used in this experiment are linearly amplified without saturation of the satellite transponders. At EAR in Indonesia, a slightly larger attenuation ratio between up and down links is statistically presented for the attenuation range of higher than 10 dB, suggesting the effects of smaller raindrop size distributions (DSD) than observed at RISH in Japan. This tendency is more conspicuous in the rainfall events when the observed attenuation shows only one peak in its time series, indicating the effects of simple convective precipitating clouds with one single cell. At RISH in Japan, a larger difference between worst month and yearly average statistics is found, due to a larger variation of the ground temperature that affects the slant-path length during the seasons, although the yearly average time percentages as such are larger at EAR than RISH up to the up-link attenuation of 15 dB. Using time percentages of their local rainfall rates, fairly good agreement is found between the observations and the ITU-R (International Telecommunication Union—Radiocommunication Sector) predictions for both locations. At EAR in Indonesia, however, the time percentages of the attenuation of more than 10 dB become significantly smaller than those predicted by the ITU-R methods for both up and down links. This indicates the remarkable reduction of equivalent path lengths down to about 2 km, caused by a fairly localized structure of convective precipitating clouds. Simultaneous X band radar observations have revealed that intense echo cores of typical rain cells causing severe attenuation

Corresponding author: Yasuyuki Maekawa, Dept. of Telecommunications and Computer Networks, Osaka Electro-Communication University, 18-8 Hatsucho, Neyagawa, Osaka 572-8530, Japan.
E-mail: maekawa@maelab.osakac.ac.jp
© 2006, Meteorological Society of Japan

¹ Present Affiliation: Kansai Branch Office, TO-DENTSU Corporation, 1-3-1 Shudocho, Chuoku, Osaka 541-0045, Japan.

are confined to about 2 km along the propagation path. This result, which seems rather small even compared with those obtained in other tropical observation sites, may be attributed to unique features of the EAR site that is located in a highland basin 865 m above the mean sea level and frequently observes simple precipitating clouds with a single cell.

1. Introduction

It is well known that rain attenuation of radio wave is significant in satellite communications using frequencies of higher than 10 GHz such as Ku band (14/12 GHz) and Ka band (30/20 GHz) (e.g., Arbesser-Rastburg and Brussaard 1993, Dintelmann et al. 1993, Bauer 1997, Karasawa and Maekawa 1997). Rain attenuation may become very severe even for Ku-band radio waves in heavy rain regions like the tropics (Pan et al. 2001, Pan and Allnut 2004). However, demand for satellite communications is recently increasing in new developing areas such as the South-East Asia, which is one of the heaviest rain regions in the world (Minakoshi et al. 2001). Ku-band radio waves thus tend to be attenuated by rain more significantly than C-band (6/4 GHz) radio waves which have been long used until now in these areas. Therefore, we need to investigate the Ku-band rain attenuation characteristics in more detail in the tropics.

In this study, we had an opportunity to monitor the signal levels received at both VSAT (Very Small Aperture Terminal) stations of the Ku-band satellite links that connect Research Institute for Sustainable Humanosphere of Kyoto University (RISH) in Japan to Equatorial Atmosphere Radar Observatory (EAR) in Indonesia (Fukao et al. 2003), using Japan's domestic communication satellite Superbird C. The observations have been continuously conducted since January 2003 at both stations. Up to now, the attenuation that has occurred in almost all rainfall events in each side has been simultaneously recorded every second at both stations for three years. Moreover, referring to the attenuation measured at the other side station under the clear sky condition together with the attenuation measured at the rainy station itself, the up-link rain attenuation which is usually difficult to detect at its own rainy station has been detected, as well as the down-link rain attenuation in both Japan and Indonesia. Thus, we have successfully obtained

fairly long-term statistics for up- and down-link rain attenuation of the Ku-band satellite communications, for the first time, in both temperate and tropical regions. Furthermore, X-band meteorological radar observations which have been also conducted at the EAR site are introduced to reveal the rain distribution of precipitating clouds at the same time in the tropics as was done in Singapore (Thurai et al. 2003).

This study presents the first quick-look report on up- and down-link rain attenuation statistics of the Ku-band satellite communications in the tropics for the past three years from January 2003 to December 2005. We here place much emphasis on difference in the rain attenuation characteristics between the temperate and tropical regions. Specifically, ratio of up-link to down-link attenuation, difference between worst month and yearly average statistics, and comparison with the recent prediction methods by ITU-R (International Telecommunication Union—Radiocommunication Sector) are discussed for the observational results obtained at both stations in Japan and Indonesia. Note that all of these problems are very important to design new Ku-band satellite communications links with large data transmission capacity in the tropics in future. Also, they are essential to investigate the effects of tropical rain characteristics on the propagation paths.

More detailed propagation-path parameters needed for actual satellite link operations, such as fade durations and intervals due to rain attenuation, will be further discussed elsewhere in the field of radio communications in future. In addition, the X-band radar observations which are only used this time to qualitatively present rain distribution along the propagation path will be further analyzed in relation to detailed rain and cloud structure in our future study.

The ITU-R prediction method (ITU-R 2003) is a representative of the methods that predict rain attenuation statistics from rainfall rate statistics at any locations. In these methods,

rain attenuation of satellite communications links that occurs along the propagation path in the air is basically predicted from rainfall rate observed on the ground. Consequently, some assumptions should be made for the rainfall structure such as homogeneity of rain distribution along the path. In this sense, a parameter called "equivalent path length" is introduced to describe an average propagation path length through a hypothetical uniform rain region that all has the same rainfall rate as observed on the ground. In the tropics, however, accuracy of these prediction models based on this equivalent path length has to be further improved because observational data for both rainfall rate and rain attenuation statistics are very sparse. Discrepancies between the ITU-R predictions and the present observations, especially found in a range of large rainfall rates with time percentages of less than 0.01%, will be examined in light of the reduction of equivalent path lengths through convective precipitating clouds which are revealed by the X-band radar observations.

As for a problem of up-link transmission power control, the ratio of up- to down-link attenuation usually expressed by the average ratio of each dB value should be obtained in advance, to compensate up-link attenuation that occurs on the path from ground to satellite. This operation is conducted by sensing down-link signal attenuation at an earth station and transmitting up-link signal power multiplied by this average attenuation ratio as a frequency scaling factor in real time. However, it is known that the attenuation ratio is significantly affected by raindrop size distribution (DSD) and considerably fluctuates from event to event according to rainfall types (Fukuchi et al. 1983, Kozu et al. 1988). Also, DSD is known to have notable seasonal and regional dependencies (Kozu et al. 2005). Hence it is essential to reveal the characteristics of the frequency ratio in the tropics, where the data for the Ku-band up-link attenuation has not yet been obtained.

On the other hand, quality of satellite link performance is sometimes evaluated by its monthly statistics as well as terrestrial links, when its operational service is provided on monthly basis. Especially in satellite links which usually show a large variation in

monthly rain attenuation statistics for both high and low attenuation ranges, a simple yearly or monthly time percentage of the rain attenuation is not sufficient for detailed evaluations of the link performance. For this purpose, a concept of "the worst month statistics" is used to handle monthly statistics efficiently. The worst month statistics consist of imaginary monthly statistics combining the largest cumulative time percentages separately taken from each monthly statistics for all the attenuation values of, say, 1–20 or 30 dB during an entire observational period. The ITU-R predictions (ITU-R 2003) also give a method to convert the yearly average statistics into the worst month statistics at any locations. But its accuracy in the tropics still has to be tested due to the lack of observational data. Therefore, the difference between the worst month and yearly average statistics is investigated in Indonesia as well as in Japan, in relation to their seasonal variations of rainfall and ground temperature.

2. Observation systems

The satellite links of Superbird C use a data transmission rate of 128 kbps, connecting RISH to EAR. At RISH, the up-link transmission carrier frequency is 14.1292 GHz and the down-link receive carrier frequency is 12.7351 GHz. At EAR, on the other hand, the up-link transmission carrier frequency is 14.4651 GHz and the down-link receive carrier frequency is 12.3992 GHz. At both stations, the up-link radio waves use the vertical linear polarization, while the down-link radio waves use the horizontal linear polarization. The elevation angle is about 49° at RISH, while it is about 39° at EAR. These specifications of the VSAT (Very Small Aperture Terminal) stations at RISH and EAR are summarized in Table 1. Although EAR is just located on the equator (0.2°S, 100.3°E), its longitude is considerably separated from the satellite orbital position (144°E). For this reason, the satellite link has a slant path with the elevation angle of about 39° even in the equatorial region instead of nearly vertical paths. The VSAT systems at both stations have an off-set Gregorian parabola dish with diameter of 1.8 m.

For our data acquisition systems, personal computers (PCs) equipped with 16-bit A/D converter boards are set up at both EAR and RISH

Table 1. Specifications of the VSAT stations at RISH and EAR

	RISH in Japan	EAR in Indonesia
Transmission frequency	14.1292 GHz	14.4651 GHz
Transmission polarization	Vertical	Vertical
Receiving frequency	12.7351 GHz	12.3992 GHz
Receiving polarization	Horizontal	Horizontal
Elevation angle	49°	39°
Height above mean sea level	50 m	865 m

stations. The PCs measure Automatic Gain Control (AGC) voltage of the In Door Unit (IDU) of the VSATs every second. The measured data is stored in their internal hard disk drives. The PCs are connected to the Internet through the satellite links, so we can remotely control them and easily execute file transfer from Osaka Electro-Communication University (OECU) in Japan. The observational time of each computer is adjusted using the clock of the workstation that controls the network systems at EAR and obtains the universal time from a GPS (Global Positioning System) receiver. An Optical Rain Gauge (ORG) was installed at EAR by a Shimane University group and we can utilize their 1-min rainfall rate data for this study. At the RISH station, we installed a rain gauge with 0.1 mm tipping buckets and started measurements of 1 min rainfall rates. The observation systems directly measure the AGC voltage, so we have to convert the voltage into received signal levels to discuss rain attenuation of the signal. We did this conversion using several samples of representative output voltage, which are calibrated over a wide range of signal levels indicated on the front panel of the IDU in dBm (Maekawa et al. 2004).

In this study, distribution of precipitating clouds just along the propagation path of the satellite radio wave is investigated using an X-band meteorological radar, which was also introduced to the EAR site by the Shimane University group. The radar has an operational frequency of 9.74 GHz and a peak transmission power of 40 kW. The diameter of the parabola dish is 1.2 m, the range resolution is 100 m, and the maximum range is 30 km. The horizontal beam scanning rate is 2 rpm, and the radar

can present CAPPI (Constant Altitude Plan Position Indicator) and RHI (Range Height Indicator) displays every 10 min using 16 elevation angles.

3. Estimation of up-link and down-link attenuation

The satellite Superbird C receives an SCPC (Single Channel Per Carrier) signal from one earth station, linearly amplifies it by a constant gain without saturation of the transponder, and transmits it to the other station. In this case, the gain of the satellite transponder is constant regardless of up-link signal strength, so we can detect up-link attenuation of one station from down-link signal strength of the other station (Hatsuda et al. 2004). Although a dynamic range of the attenuation measurements depends on a clear sky level, we can usually estimate rain attenuation down to 20 dB. This dynamic range as such is slightly smaller than that of satellite beacon or broadcasting channel measurements, which sometimes extend to more than 30 dB. But as will be shown later in Chapter 5, it is still large enough to detect the rain attenuation with time percentages of down to 0.001% in Ku band.

The clear sky level at each station is, on the other hand, determined by the signal levels received in the conditions when rainfall rate is recorded at neither RISH in Japan nor EAR in Indonesia on hourly basis. Since the clear sky level in itself shows a distinct diurnal variation with amplitude of 1–2 dB due primarily to the fluctuation of the satellite attitude, it is calculated for each local time using hourly values averaged over a few days before and after the respective rainfall events at both stations. The

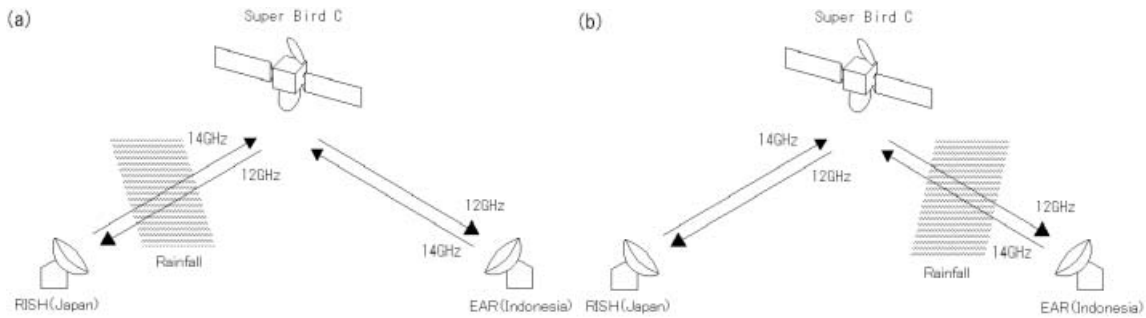


Fig. 1. Methods of up- and down-link attenuation measurements when rain is falling at (a) RISH in Japan and (b) EAR in Indonesia.

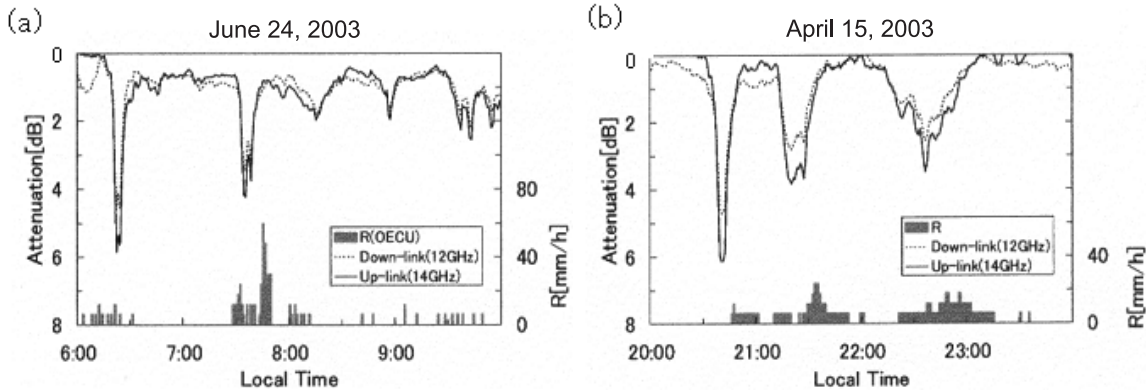


Fig. 2. Examples of up- and down-link attenuation that occurred at (a) RISH in Japan and (b) EAR in Indonesia.

rain attenuation is then estimated every minute by the difference between the signal levels received in each rain event and those interpolated from the hourly clear sky levels determined on the other rain-free days before and after the event.

Figure 1 shows examples of the observational methods when it is raining at (a) RISH in Japan and (b) EAR in Indonesia, respectively. When rain is falling in Japan as shown in Fig. 1(a), down-link attenuation is directly measured by the down-link signal strength received at RISH. At the same time, up-link attenuation at RISH is estimated from the down-link signal strength received by its opposite terminal at EAR in Indonesia. When rain is falling in Indonesia as shown in Fig. 1(b), on the other hand, down- and up-link attenuation is measured at EAR and RISH, respectively. The occurrence of rainfall was easily detected by records of the rain gauge installed at or near each station.

Fortunately, peaks of rainy seasons are slightly shifted between Japan and Indonesia as will be shown later, so time percentages of simultaneous occurrence of heavy rain such as more than 20 mm/h are less than 0.001%, being quite negligible for the Ku-band rain attenuation discussed in this study.

Figure 2 shows examples of up- and down-link rain attenuation which were measured at (a) RISH and (b) EAR, respectively, by simultaneously monitoring signal levels at both stations in Japan and Indonesia. The solid and dashed lines indicate the up- and down-link attenuation, respectively. Each data point is based on 1-min averaged attenuation values. The bar chart at the bottom of the figure depicts 1-min rainfall rates. In these rain events, the up- and down-link attenuation reaches about 6 and 5 dB, respectively, at both stations. Note that the up link in 14 GHz band indicates by about 10–20% larger attenuation than the

down link in 12 GHz band due to its higher frequency. Thus, the rain attenuation of the up and down links is successfully detected at both stations in Japan and Indonesia by our observational methods proposed in Fig. 1. The observational result suggests that this technique should be further applied to other earth stations using Ku-band SCPC signals in both temperate and tropical regions, to collect up- and down-link attenuation statistics of wider areas in future.

4. Ratio of up-link to down-link attenuation

4.1 Frequency scaling factors for various attenuation ranges

The relationships between up-link (14 GHz) and down-link (12 GHz) attenuation observed at both stations are here investigated in light of the ratio of their dB values. Also, a frequency scaling factor given by this average ratio to cope with up-link rain attenuation in actual satellite link operations is discussed, in relation to kinds of raindrop size distributions (DSD) for various attenuation ranges. First, scatter plots of up-link attenuation against down-link attenuation are shown in Fig. 3, for the rainfall events that occurred at (a) RISH in Japan and (b) EAR in Indonesia in 2004. At each station, these rainfall events are primarily taken from

rainy seasons that produce large attenuation of more than 10 dB. The months corresponding to their rainy seasons are from May to October for RISH (Japan), and February–May and October–December for EAR (Indonesia), respectively, in 2004. Three thin lines are theoretical relationships of the frequency scaling between up- and down-link attenuation at each station (Iida 1997). These theoretical values are based on the three typical kinds of raindrop size distributions such as Joss-drizzle (Jd), Marshall-Palmer (MP) and Joss-thunderstorm (Jt) types (Joss and Waldvogel 1969, Marshall and Palmer 1948), assuming homogeneity of rain along the path. The equivalent path length needed for this theoretical calculation is, on an average, assumed to be 4 and 3 km at RISH (Japan) and EAR (Indonesia), respectively, for the large attenuation range of more than 10 dB, as will be shown in Fig. 10 in Chapter 6. It is found from Fig. 3 that the data points observed at both station exist around these three theoretical values, although they are considerably scattered.

More specifically in Fig. 3(a), the data points observed at RISH are centered around the Jd type up to 10 dB down-link attenuation except for a small attenuation range of less than about 3 dB, while they approach the Jt type in a large attenuation range of more than 10 dB. These

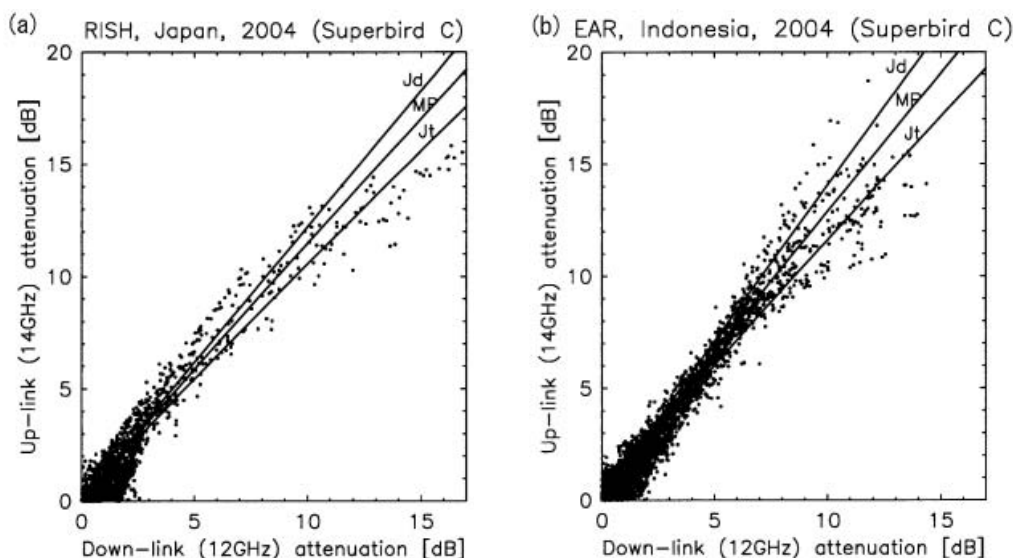


Fig. 3. Scatter plots of up-link against down-link attenuation observed in rainy seasons of the year 2004 at (a) RISH in Japan and (b) EAR in Indonesia.

tendencies in small (<3 dB), middle (3–10 dB) and large (>10 dB) attenuation ranges are very similar to those found in the long term frequency scaling statistics between Ka-band N-Star beacon signal (19.45 GHz) rain attenuation and Ku-band BS broadcasting signal (11.84 GHz) rain attenuation at Neyagawa, Osaka in Japan (Karasawa and Maekawa 1997). The frequency scaling relationship between N-Star and BS was, however, obtained from the equi-probability values of their attenuation measured in different propagation paths and observational instances, while the present relationship between up- and down-link attenuation is detected directly from the instantaneous observational values measured on the same propagation path at the same time. Hence, these results on the frequency scaling between the Ku-band up and down links of Superbird C are considered to have more realistic physical meanings.

In Fig. 3(b), on the other hand, the data points observed at EAR in Indonesia distribute around the Jd type in the middle attenuation range of 3–10 dB in the same way as at RISH in Japan. Some of them, however, still stay around the Jd type even in the large attenuation range of more than 10 dB, instead of approaching the Jt type on the whole as was observed in Japan. Consequently the data points are rather centered around all of the three typical DSDs in a larger attenuation range, giving rise to a slightly larger frequency scaling factor

(average attenuation ratio) between up and down links at EAR in Indonesia than at RISH in Japan.

4.2 Frequency scaling factors for single or multiple cell clouds

Next, a rainfall type which produces a larger frequency scaling factor is investigated on event-to-event basis at EAR in Indonesia. Figure 4 shows examples of rainfall events with considerably large up- and down-link rain attenuation observed on (a) March 29 and (b) May 2, 2004, respectively. These events are depicted by scatter plots of the up- and down-link attenuation, together with their time variation and rainfall rate at 1 min interval during three hours in the two right-hand-side panels. The solid and dashed lines indicate up- and down-link attenuation, respectively. On March 29 in Fig. 4(a), large up-link attenuation of more than 5 dB are observed three times during about one hour period. At the same time we can see three rainfall rate peaks of more than 60 mm/h. In this event, the ratio of the up- to down-link attenuation decreases significantly as the up-link attenuation exceeds 10 dB. The kind of DSD thus seems to change from Jd type to Jt type as the attenuation becomes large. On May 2 in Fig. 4(b), on the other hand, large up- or down-link attenuation of more than 10 dB is observed only once during three hours. In this event, the attenuation ratio remains in a larger value even in the large at-

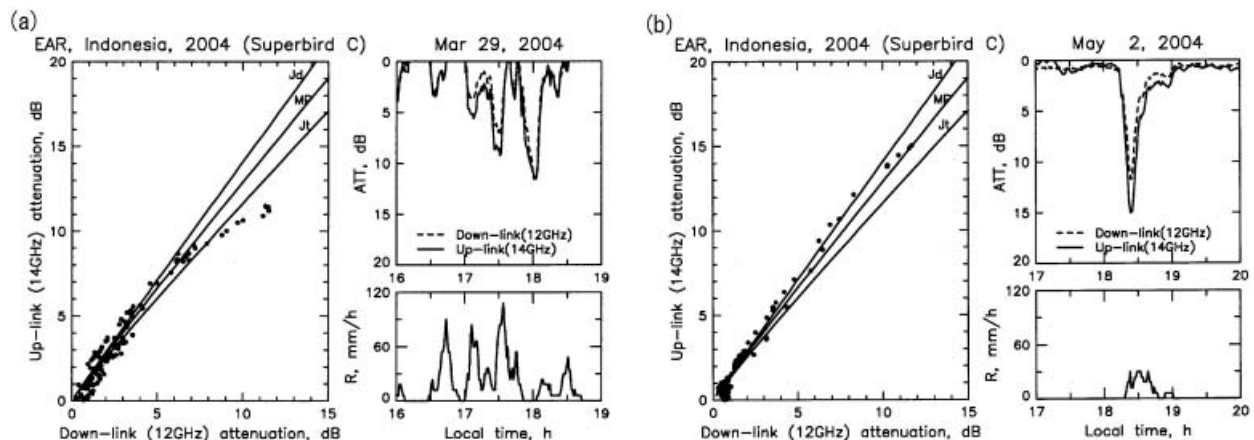


Fig. 4. Examples of scatter plots between up- and down-link attenuation observed on (a) March 29, 2004 and (b) May 2, 2004 at EAR in Indonesia.

attenuation range of more than 10 dB. The kind of DSD thus seems to stay in the Jd type up to the large rain attenuation range.

With these investigations, the latter type of event with the larger frequency scaling factor even in the larger attenuation range is possibly due to a simple convective precipitating cloud with one single cell, while the former type of events with the smaller frequency scaling factor is due to more complicated multiple clouds with larger horizontal scale. Simultaneous X-band radar observations also support these results, that is, three or more cores with intense radar echoes are detected around 17–18 LT on March 29, whereas only one intense echo core is found around 18–19 LT on May 2, 2004 on the CAPPI display. Furthermore, these tendencies are similarly found without exception in almost all rainfall events observed in 2004. Figure 5 shows scatter plots of up-link against down-link attenuation for (a) events with only one peak of the attenuation and (b) those with more than two peaks of the attenuation, respectively, both of which occurred during the one year of 2004. The number of their events is 23 and 26 for (a) and (b) in Fig. 5, respectively. Thus, it is statistically seen from Fig. 5(a) that the large frequency scaling factor up to the

large attenuation values is primarily attributed to the events with only one peak of attenuation. On the other hand, Fig. 5(b) indicates that the ratio of the up- to down-link attenuation becomes significantly smaller in the large attenuation range of more than 10 dB, yielding the almost same tendency of the frequency scaling factors as shown in Fig. 3(a) for RISH in Japan. Therefore, one possible cause of the comparatively larger frequency scaling factor of the attenuation at EAR should be attributed to isolated simple convective precipitating clouds with one single cell, which is peculiar to the tropics and not frequently observed at RISH in Japan.

The simultaneous X-band radar observations also reveal on the RHI displays, as will be shown later, that height of the rain cells with intense radar echoes is usually lower than 4 km above the ground level at EAR for both isolated single clouds and complicated multiple clouds, and that these convective clouds are not usually accompanied by a bright band which is caused by a melting layer. Thus in the tropical rainfall events that produce large attenuation, the effects of bright bands on the attenuation ratio between up and down links are considered to be negligible (Kozu et al. 1988), and their fre-

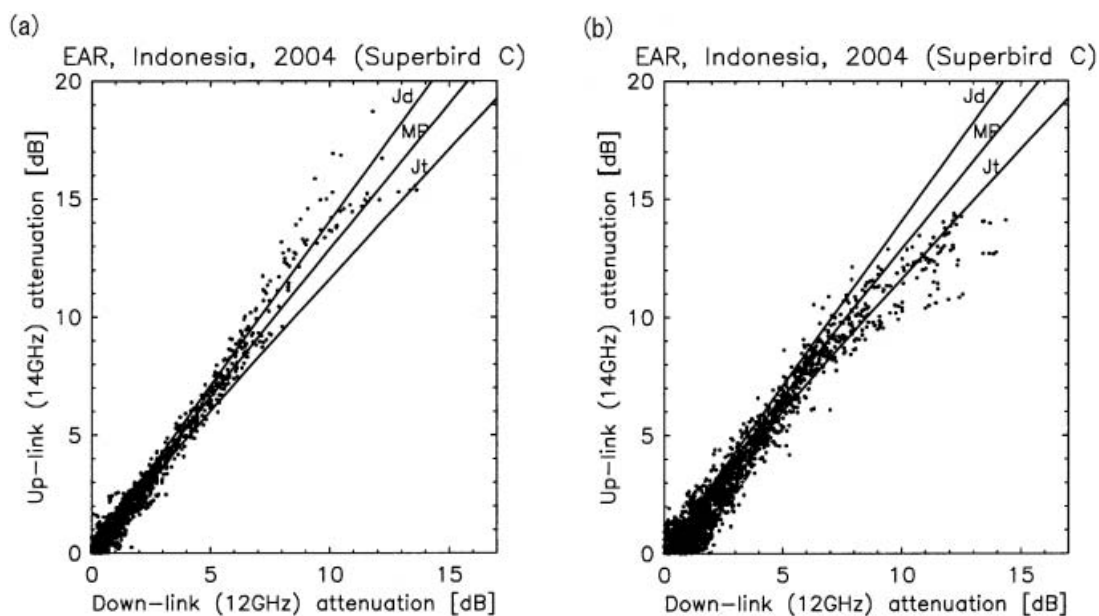


Fig. 5. Scatter plots of up-link against down link attenuation for (a) events with only one peak of attenuation and (b) those with more than two peaks of attenuation at EAR.

quency scaling factors are primarily determined by DSD in the rain cells. On the other hand, reasons why the convective clouds with one single cell produce comparatively smaller DSD and larger frequency factors are not yet made clear. Considering that they generally have shorter life time and smaller horizontal scales on the CAPPI display, however, their convective activities are possibly expected to be weaker than the clouds with multiple cells that may develop and sustain comparatively larger DSD easily. Furthermore, the relationship between the kind of convective cells and the frequency scaling factor seems to be universally found in nearly fifty rainfall events in 2004. These features should be further investigated in future in light of the development of convective clouds and DSD using time series of the CAPPI displays and DSD measurements at EAR.

5. Rain attenuation statistics

5.1 Worst month and yearly average statistics

Figure 6 shows worst month statistics and yearly average cumulative time percentages for up-link attenuation at (a) RISH in Japan and (b) EAR in Indonesia, respectively. The observational period is three years from January 2003 to December 2005. Also, Fig. 7 indicates their relationships in the form of logarithmic

scale for the up-link attenuation observed at (a) RISH and (b) EAR. It is found that the relationships between the worst month and yearly average statistics are almost linear in the logarithmic scale at both stations except for extremely small yearly average time percentages of less than 0.01% at EAR, so they are represented by the following formula:

$$P = aP_w^b \tag{1}$$

where P_w and P are the worst month and yearly average cumulative time percentages, respectively; a and b are co-efficients for the least RMS (Root Mean Square) fitted approximation lines shown by the dashed lines in Fig. 7. These best fitted parameters for Eq. (1) are given by $a = 0.17$ and $b = 1.14$ at RISH in Japan; $a = 0.34$ and $b = 1.16$ at EAR in Indonesia, respectively. As for the down-link attenuation statistics, the almost same values are obtained for the parameters of a and b at both RISH and EAR.

The ITU-R prediction method recommends the values of $a = 0.30$ and $b = 1.15$ in Eq. (1) for global planning purposes (ITU-R 2003, Iida 1997), presenting a slightly larger and smaller value for the parameter a than those observed at RISH and EAR, respectively, whereas the parameter b recommended by the ITU-R method is almost the same as those observed

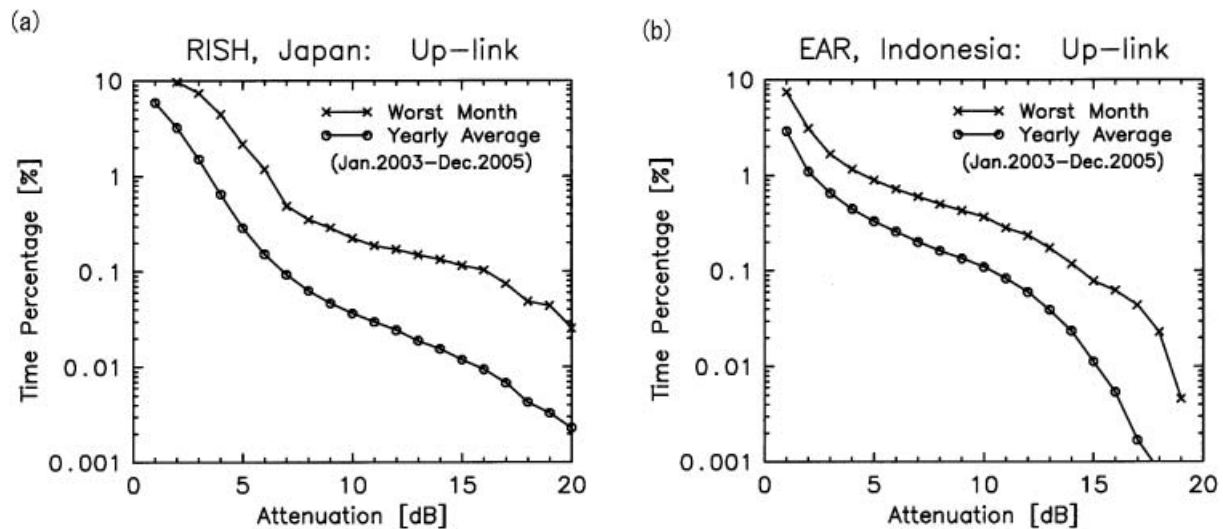


Fig. 6. Worst month and yearly average cumulative time percentages for up-link attenuation observed at (a) RISH and (b) EAR from January 2003 to December 2005.

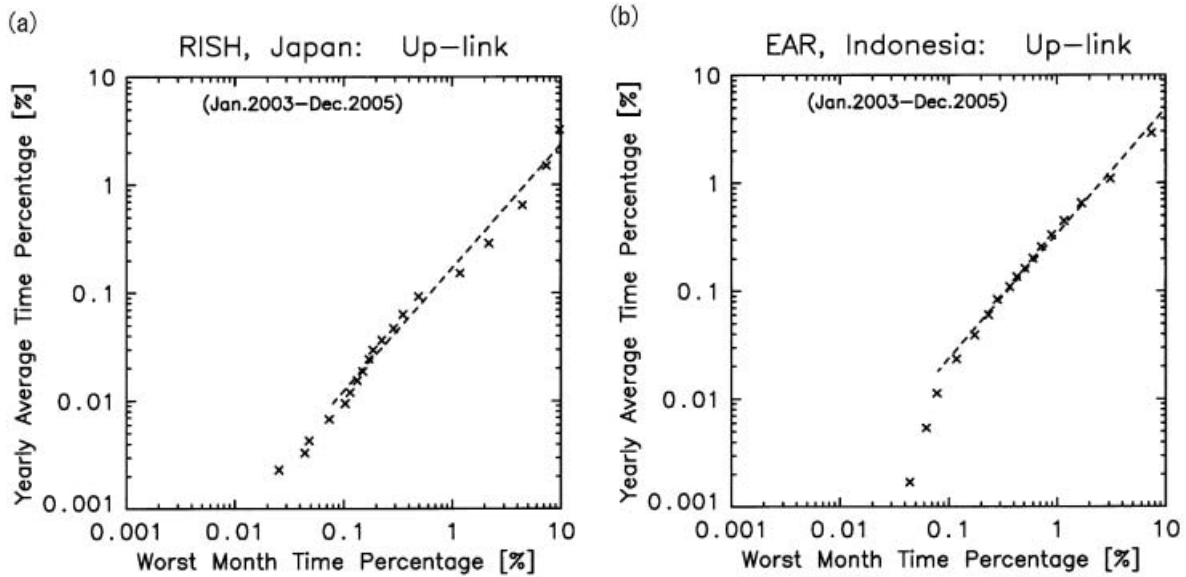


Fig. 7. Relationship between worst month and yearly average cumulative time percentages or up-link attenuation observed at (a) RISH and (b) EAR.

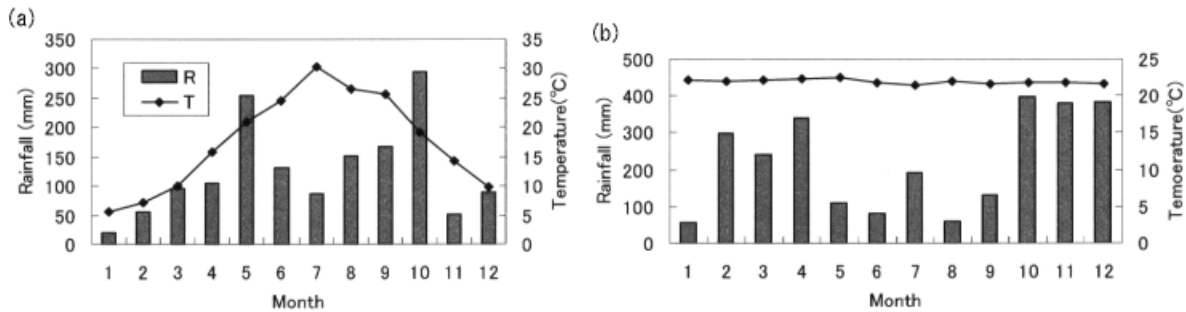


Fig. 8. Monthly rainfall and average ground temperature obtained in 2004 at (a) RISH in Japan and (b) EAR in Indonesia.

at both stations. It should be noted that as the parameter a becomes smaller than one, the difference between the worst month and yearly average statistics becomes larger, so the smaller value of the parameter a means the larger difference of these statistical characteristics at RISH in Japan. This is primarily caused by a larger seasonal variation of their monthly cumulative time percentages in Japan.

5.2 Seasonal variation of rainfall and ground temperature

Figure 8 depicts monthly rainfall and average ground temperature obtained in 2004 at (a) RISH and (b) EAR, respectively. Figure 8

also indicates that seasonal variation of the ground temperature is much larger in Japan, whereas it is almost constant during the whole seasons in Indonesia. This suggests a much larger change of rain height during the year in Japan (Fujita et al. 1979). Therefore, the change of slant-path length of the radio wave through rain height, as well as the monthly rainfall, causes the larger seasonal variation of the monthly statistics and the larger difference between the worst month and yearly average statistics in Japan. It should be also noted that the rainfall in May and October is exceptionally large due to the unusual approach of typhoons to Japan in these seasons. In Indonesia, on the

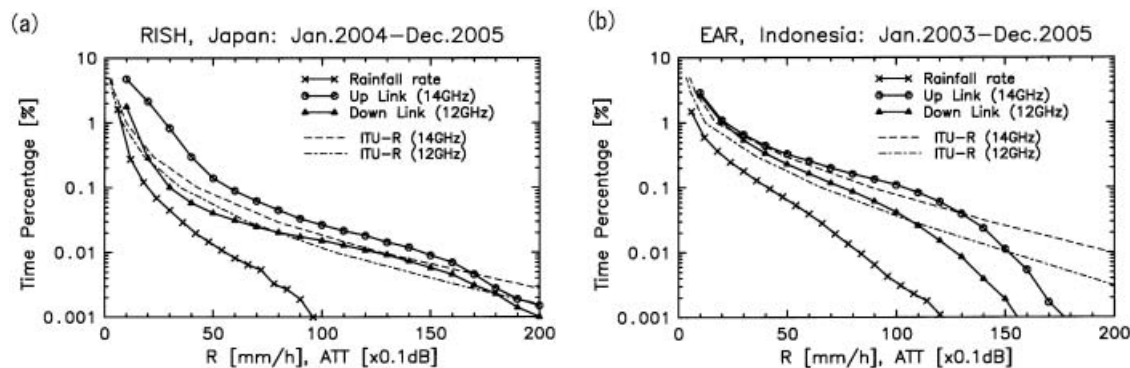


Fig. 9. Yearly average statistics of up- and down-link rain attenuation and rainfall rate observed at (a) RISH and (b) EAR, together with the ITU-R predictions (2003).

other hand, the rain height given by 0°C height becomes nearly constant during the year. Also, the total rainfall in 2004 is significantly larger in Indonesia than in Japan, which is specifically about 2700 mm at EAR in Indonesia and about 1500 mm at RISH in Japan, respectively. However, its effects on the seasonal variation of the rain attenuation statistics, such as the worst month statistics, are found to be rather smaller at EAR.

5.3 Comparison with rainfall rate statistics

Next, Fig. 9 shows the average cumulative time percentages of the up- and down-link rain attenuation and those of the rainfall rates measured for two and three years at (a) RISH in Japan and (b) EAR in Indonesia, respectively. The rainfall rate measurement at RISH has started since 2004. Also shown are the prediction values for the up- and down-link attenuation based on the recent ITU-R recommendations by dashed (14 GHz) and dashed-dotted (12 GHz) lines, respectively. The rainfall rates for the cumulative time percentage of 0.01% used in the ITU prediction method (ITU-R 2003) are 60 mm/h and 85 mm/h at RISH and EAR, respectively. As a whole, good agreement is found between the measurements and the predictions. At RISH in Japan, the time percentages of the up- and down-link attenuation fairly well follow the ITU-R predictions up to 20 dB attenuation. At EAR in Indonesia, on the other hand, they become much smaller than the ITU-R predictions and rapidly decrease down to 0.001% as the attenuation exceeds 10 dB. Moreover, the time percentages

become even smaller than those observed at RISH in Japan as the attenuation becomes larger than about 15 dB, although the rainfall rate in itself remains much larger than at RISH down to 0.001% time percentage. This may represent a fairly localized structure of convective precipitating clouds along the slant path in the tropics for these heavy rainfall rates of more than, say, 85 mm/h which corresponds to 0.01% time percentage or less.

6. Equivalent path length

6.1 Equi-probability relationship between rainfall rate and attenuation

Figure 10 shows equi-probability values of the up-link attenuation against the rainfall rates obtained at (a) RISH and (b) EAR for the past two and three years, respectively. Solid and dashed lines indicate theoretical relationships between attenuation and rainfall rates for equivalent path lengths of 2–6 km. In these calculations, the raindrop size distribution (DSD) is based on the Marshall-Palmer type (Iida 1997). At RISH in Japan, the equivalent path length estimated from these theoretical lines in Fig. 10(a) remains more than 4 km up to the rainfall rate of 60 mm/h, whereas it slightly decreases down to 3 km as the rainfall rate exceeds 60 mm/h. This equivalent path length of more than 4 km agrees well with that previously obtained by the CS propagation experiments up to 50 mm/h at Kashima, Ibaraki in Japan (Fukuchi et al. 1983). At EAR in Indonesia, however, the equivalent path length estimated in Fig. 10(b) rapidly decreases down to 2 km as the rainfall rate reaches 130 mm/h,

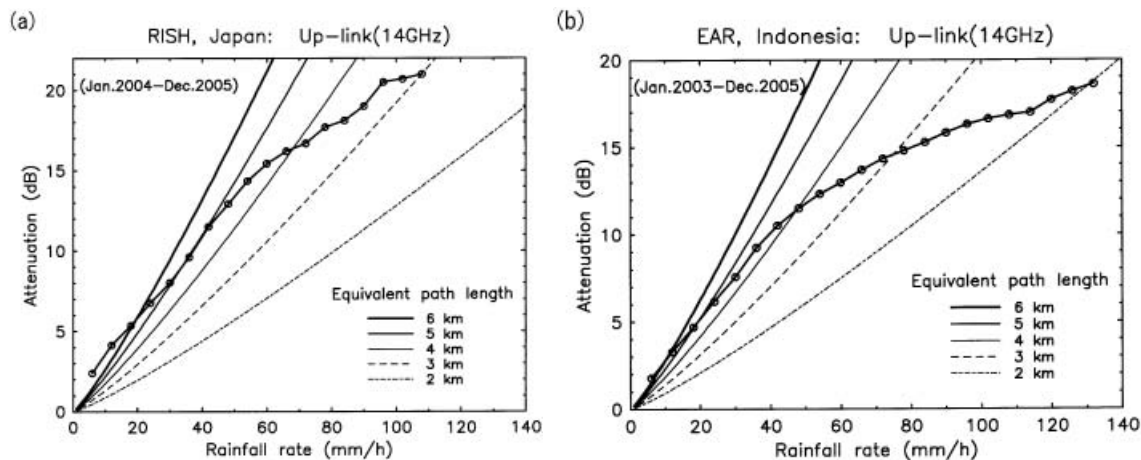


Fig. 10. Equi-probability values of up-link attenuation against the rainfall rates obtained at (a) RISH and (b) EAR.

although it remains more than 3 km below 60 mm/h. These features of the equivalent path lengths are also obtained for the down-link attenuation at both stations.

The equivalent path length of as short as 2 km for such heavy rainfall rates obtained at EAR thus suggests a localized structure of the convective precipitating clouds causing severe attenuation. Note that the EAR site is located in a highland basin 865 m above the mean sea level as shown in Table 1, so this may yield a cloud top or rain height above the ground level slightly lower than those obtained from lowland plains near the mean sea level in severe rainstorms. Also, the isolated clouds with a single cell frequently observed at EAR tend to produce shorter equivalent path lengths in light of their small horizontal structure for the elevation angle of about 39° . Thus, these unique features obtained at the EAR site, such as comparatively lower cloud tops due to a highland and their simple horizontal structure, may explain the rapid decreases of the equivalent path length and the time percentages above 10 dB attenuation shown in Figs. 9 and 10. In deed, this tendency is more conspicuous than those observed in other tropical locations such as in Bandung, Indonesia (Sastrokusumo et al. 2001) and in Lae, Papua New Guinea (Pan et al. 2001). The equivalent path lengths deduced from equi-probability relationship between their cumulative time percentages of rainfall rate and attenuation are kept around

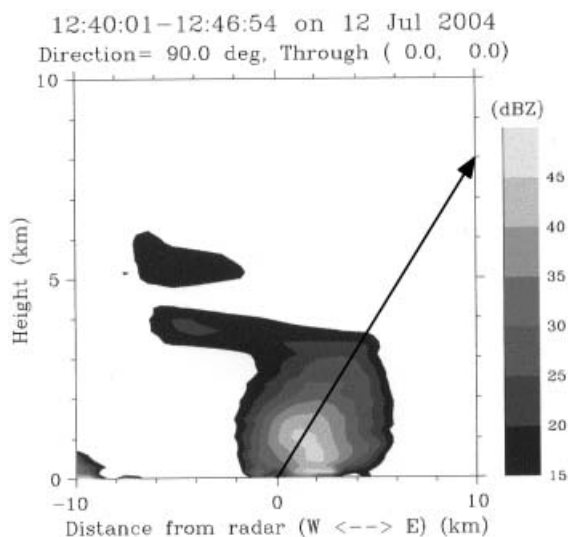


Fig. 11. Example of X-band radar echo distribution along the path of the satellite link indicated by an arrow.

3 km up to the attenuation of more than 10 dB in both locations.

6.2 Radar observations of the rain along the propagation path

Figure 11 shows an example of radar echo distribution along the propagation path observed in the convective rainstorm on July 12, 2004. The radar echoes are depicted on the RHI display in the east-west direction, including the propagation path of the satellite link

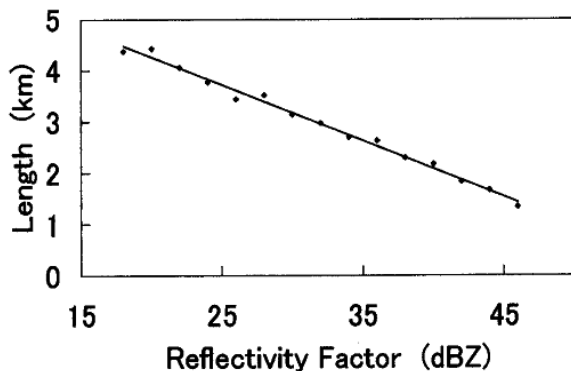


Fig. 12. Average lengths of radar echo distribution along the path according to the echo intensities.

that is indicated by an arrow in Fig. 11. It is found that intense echoes of more than 45 dBZ are confined to about 2 km around the core of the cloud. Note that the size of this core is about 2 km in both horizontal and vertical dimensions. The distribution of radar echoes along the propagation path has been further accumulated for the convective clouds observed during one year from 2003 October to 2004 September. In Fig. 12, average lengths of the cloud cores are classified according to the radar echo intensities surrounding the cores along the propagation path indicated by the arrow in Fig. 11.

Figure 12 indicates that the path lengths across cloud cores with weak echo intensities around them extend beyond 4 km, whereas the path length with intense echoes is reduced down to around 2 km. Thus, we can see a tendency that the cloud core size remarkably reduces with increasing radar echo intensities, being similar to that of the equivalent path length shown in Fig. 10(b). In Fig. 12, however, the average length of the cloud cores along the propagation path just means a dimension that simply exceeds the specified radar reflectivity factors averaged over 10 min, so this length is not directly equated to the equivalent path length estimated by the equi-probability relationship between 1-min ground rainfall rate and path-integrated rain attenuation in Fig. 10(b). Nevertheless, the results of these simultaneous radar observations still seem to support the fact that the size of intense rain cells

along the propagation path is eventually reduced down to about 2 km as the rainfall rate extremely increases, and can qualitatively explain the remarkable reduction of the equivalent path lengths detected at EAR in the tropics.

7. Conclusions

In this study, the observation technique to measure the rain attenuation of both up and down Ku-band satellite links has been, for the first time, introduced to the VSAT systems in the tropical region, using two SCPC signal levels of Superbird C received in Japan and Indonesia, respectively. The up-link attenuation is, in general, found to be by about 10–20% larger than the down-link attenuation, being in fairly good agreement with the frequency scaling models using three typical raindrop size distributions. Thus, the first systematic data base of both up- and down-link attenuation has been obtained for the past three years in the tropics. The primary results on the tropical rain attenuation statistics different from those of the temperate region are as follows.

- (1) At EAR in Indonesia, the attenuation ratio is slightly larger in the severe attenuation range of more than 10 dB. This larger ratio is shown to be primarily caused by simple convective clouds with one single cell possibly accompanied by smaller raindrop size distributions.
- (2) The yearly average time percentages of the up-link attenuation up to 15 dB are larger than those obtained at RISH in Japan, due to the larger annual rainfall. The difference between worst month and yearly average statistics is, however, rather smaller due to the lack of the seasonal variation of the ground temperature that causes the change of the path length.
- (3) The yearly average attenuation statistics are in fairly good agreement with the ITU-R predictions (2003) up to 10 dB for both up- and down-link attenuation. In the attenuation of more than 10 dB, however, the time percentages become much smaller than the predictions, indicating the remarkable reduction of the equivalent path length down to about 2 km. The radar observations also suggest that intense echo cores of

the simple convective clouds causing the severe rain attenuation which are frequently detected in this experiment in a highland basin are confined to 2 km along the propagation path.

Further observations are, of course, needed to investigate year-to-year variation of rain attenuation statistics and its relation with yearly anomalies of the equatorial climate. In addition to the X-band meteorological radar partly introduced in this study, a number of observations of clouds and hydrometeors are now being conducted by various instruments, such as a 2-dimensional video disdrometer, a radiometer, and so on at the EAR site, as well as atmospheric motions by EAR itself. In future, more detailed rain attenuation characteristics such as duration time and space and time diversity effects are required to be analyzed in light of horizontal and height distributions of precipitating clouds obtained at the same time from these remote sensing techniques.

Acknowledgements

The authors deeply thank the staff of Equatorial Atmosphere Radar Observatory for assisting our study and observations. This work is supported by Grant-in-Aid for Scientific Research on Priority Area-764 of the Ministry of Education, Culture, Sports, Science and Technology of Japan (Grant No.14213201).

References

- Arbesser-Rastburg, B.R. and G. Brussaard, 1993: Propagation research in Europe using the OPYMPUS satellite. *Proc. IEEE*, **81**, 865–875.
- Bauer, R., 1997: Ka-band propagation measurement: An opportunity with advanced communication technology satellite (ACTS). *Proc. IEEE*, **85**, 853–862.
- Dintenmann, F., G. Ortgies, F. Ruecker, and R. Levis, 1993: Results from 12- to 30-GHz German propagation experiments carried out with the OLYMPUS satellite. *Proc. IEEE*, **81**, 876–884.
- Fujita, M., K. Nakamura, T. Ihara, and R. Hayashi, 1979: Seasonal variation of attenuation statistics in millimetre-wave earth-satellite link due to bright band height. *Elletron. Lett.*, **15**, 654–655.
- Fukao, S., H. Hashiguchi, M. Yamamoto, T. Tsuda, T. Nakamura, M.K. Yamamoto, T. Sato, M. Hagio, and Y. Yabugaki, 2003: The Equatorial Atmosphere Radar (EAR): System description and first results. *Radio Sci.*, **38**, 1053, doi:10.1029/2002RS002767.
- Fukuchi, H., T. Kozu, K. Nakamura, J. Awaka, H. Inomata, and Y. Otsu, 1983: Centimeter wave propagation experiments using the beacon signals of CS and BSE satellite. *IEEE Trans. Antennas and Propagat.*, **31**, 603–613.
- Hatsuda, K., Y. Aoki, H. Echigo, F. Takahata, Y. Maekawa, and K. Fujisaki, 2004: Ku-band long distance site-diversity (SD) characteristics by using new measuring system. *IEEE Trans. Antennas and Propagat.*, **52**, 1481–1491.
- Iida, T., 1997: *Satellite Communications (in Japanese)*, Ohmsha, 427p.
- ITU-R, 2003: P837-1 Characteristics of precipitations for propagation modeling. *ITU-R Recommendations*.
- Joss, J. and A. Waldvogel, 1969: Raindrop size distribution and sampling size errors. *J. Atmos. Sci.*, **26**, 566–569.
- Karasawa, Y. and Y. Maekawa, 1997: Ka-band earth-space propagation research in Japan. *Proc. IEEE*, **85**, 821–842.
- Kozu, T., J. Awaka, H. Fukuchi, and K. Nakamura, 1988: Rain attenuation ratios on 30/20- and 14/12-GHz satellite-to-earth paths. *Radio Sci.*, **23**, 409–418.
- , T. Shimomai, Z. Akramin, Mazuki, Y. Shibagaki, and H. Hashiguchi, 2005: Intra-seasonal variation of raindrop size distribution at Koto Tabang, West Sumatra. *Geophys. Res. Lett.*, **32**, L07803, doi:10.1029/2004GL022340.
- Maekawa, Y., T. Fujiwara, Y. Shibagaki, T. Sato, M. Yamamoto, H. Hashiguchi, and S. Fukao, 2004: First year results on rain attenuation characteristics of satellite links at equatorial atmospheric radar. *Proc. 2004 IEEE AP-S International Symposium*, **2**, 1660–1663.
- Marshall, J.S. and W.M. Palmer, 1948: The distribution of raindrop with size. *J. Meteor.*, **5**, 165–166.
- Minakoshi, H., K. Igarashi, T. Boonchouk, N. Hemmakorn, A. Yagasena, S.I. Hassan, J. Suryana, U. Sastrokusumo, S.C.N. Monje, and R. Reyes, 2001: Rain attenuation measurements in Ku-band satellite communication in the East-Asian region under the POST-PARTNERS project. *2001 Asia-Pacific Radio Science Conference, Digest*, **1**, 153, F1-2-01.
- Pan, Q.W., G.H. Bryant, J. McMahan, J.E. Allnutt, and F. Haidara, 2001: High elevation angle satellite-to-earth 12 GHz propagation measurements in the tropics. *International Journal of Satellite Communications*, **19**, 363–384.
- and J.E. Allnutt, 2004: 12-GHz fade durations

- and intervals in the tropics. *IEEE Trans. Antennas and Propagat.*, **52**, 693–701.
- Sastrokusumo, U., H. Wundarto, J. Suryana, K. Igarashi, and H. Minakoshi, 2001: Two years rainfall rate and rain attenuation measurements in Indonesia under the POST-PARTNERS Project. *2001 Asia-Pacific Radio Science Conference, Digest*, **1**, 153, F2-3-05.
- Thurai, M., T. Iguchi, T. Koizu, J.D. Eastment, C.L. Wilson, and J.T. Ong, 2003: Radar Observations in Singapore and their implications for the TRMM precipitation radar retrieval algorithms. *Radio Science*, **38**, 1086, doi:10.29/2002RS002855.